

# Noise bias in weak lensing shape measurements

Alexandre Refregier,<sup>1</sup> Tomasz Kacprzak,<sup>2</sup> Adam Amara,<sup>1</sup> Sarah Bridle,<sup>2</sup>  
Barnaby Rowe<sup>2,3,4</sup>

<sup>1</sup>*Institute for Astronomy, ETH Zurich, Wolfgang-Pauli-Strasse 27, CH-8093 Zurich, Switzerland*

<sup>2</sup>*Department of Physics & Astronomy, University College London, Gower Street, London, WC1E 6BT*

<sup>3</sup>*Jet Propulsion Laboratory, California Institute of Technology, 4800 Oak Grove Drive, Pasadena, CA 91109, USA*

<sup>4</sup>*California Institute of Technology, 1200 East California Boulevard, Pasadena, CA 91106, USA*

23 March 2012

## ABSTRACT

Weak lensing experiments are a powerful probe of cosmology through their measurement of the mass distribution of the universe. A challenge for this technique is to control systematic errors that occur when measuring the shapes of distant galaxies. In this paper we investigate noise bias, a systematic error that arises from second order noise terms in the shape measurement process. We first derive analytical expressions for the bias of general Maximum Likelihood estimators (MLEs) in the presence of additive noise. We then find analytical expressions for a simplified toy model in which galaxies are modeled and fitted with a Gaussian with its size as a single free parameter. Even for this very simple case we find a significant effect. We also extend our analysis to a more realistic 6-parameter elliptical Gaussian model. We find that the noise bias is generically of the order of the inverse-squared signal-to-noise ratio (SNR) of the galaxies and is thus of the order of a percent for galaxies of SNR of 10, i.e. comparable to the weak lensing shear signal. This is nearly two orders of magnitude greater than the systematics requirements for future all-sky weak lensing surveys. We discuss possible ways to circumvent this effect, including a calibration method using simulations discussed in an associated paper.

**Key words:** methods: statistical – techniques: image processing – cosmology: observations – gravitational lensing: weak – dark matter – dark energy

## 1 INTRODUCTION

Weak gravitational lensing is a technique to map the distribution of dark matter in the universe (see e.g. Refregier 2003; Hoekstra & Jain 2008, for reviews). It relies on measurement of the apparent shapes of distant galaxies that are distorted due to matter inhomogeneities along the line of sight. Weak lensing offers great prospects for the measurement of cosmological parameters (Peacock & Schneider 2006; Albrecht et al. 2006). In particular, the measurements of dark energy parameters with future wide field surveys is very promising but places strong requirements on weak lensing measurements and in particular in the control of systematics.

The main potential systematic effects are generally considered to be: (i) galaxy shape measurement from galaxy images; (ii) galaxy distance measurement using photometric redshifts; (iii) galaxy intrinsic alignments arising from the galaxy formation process; (iv) accuracy of theoretical predictions of dark matter clustering. We focus on the first of these in this paper.

In most cases the gravitational lensing effect produces

a matrix distortion stretching of the galaxy image. This image shear must be uncovered in the presence of nuisance observational effects, including: image blurring due to the atmosphere and telescope optics; image pixelisation due to the nature of photon detectors; and noise due to the finite number of photons from the galaxy and other backgrounds. Furthermore, the intrinsic properties of the galaxy prior to lensing distortion are unknown.

The first detection of this shearing effect was made by Tyson et al. (1990) and repeated by Bonnet et al. (1994) who also developed methods for removing the image convolution effects. This was taken to a new level by Kaiser et al. (1995) in a method that is widely referred to as KSB and that has remained the most widely used shear measurement method to this day. Essentially the KSB method uses weighted quadrupole moments of images to calculate shears, and corrects the shears for the weighting function. This was further improved in (Kaiser 2000). An alternative approach using a simple galaxy model to forward fit the data was proposed in Kuijken (1999) and implemented in Bridle et al. (2002) and Miller et al. (2007). More flexible models using Gauss-Laguerre polynomials, or shapelets, have also

been proposed (Bernstein & Jarvis 2002; Refregier & Bacon 2003). Each of these approaches has potential strengths and drawbacks. For instance the limitations of model-fitting methods were explored in Melchior et al. (2010) and Voigt & Bridle (2010), and potentially mitigated by Bernstein (2010).

There have been several simulation challenges to assess how well current methods can measure gravitational shear and to encourage development of new methods. The Shear TESting Program (STEP) 1 Challenge provided a suite of simulated images using relatively simple galaxy models but a realistic image blurring model. The galaxies were distributed with random positions across the image and the same shear was used to distort every galaxy in a given large image. It was found that the existing methods that had already been applied to observational data were sufficiently good to merit the science results on that data (Heymans et al. 2006).

The STEP2 Challenge used more realistic galaxy models and a wider range of blurring models (Massey et al. 2007) and reached similar conclusions despite this additional complexity. However, neither challenge was sufficiently large to forecast the efficacy of existing methods for use on future surveys, and neither challenge was able to address *all* potential sources of measurement bias in real data (such as uncertainty about the image Point Spread Function or PSF; see, e.g., Paulin-Henriksson et al. 2008, 2009; Rowe 2010). In addition, while it was possible in many cases to positively detect biases in weak lensing shape measurement methods, due to the complexity and realism of the STEP challenges it was not always possible to attribute definite causes for these effects. In the complex, multi-stage analysis required for weak lensing measurement it can be very difficult to isolate individual causes of systematic bias, and yet diagnosing these individual contributions is an important ongoing process in the development of accurate measurement methodology.

The GRavitational lEnsing Accuracy Testing 2008 (GREAT08) Challenge was much simpler: it reverted to simpler galaxy models; avoided overlapping galaxies; and used similar properties for all galaxies in a large image (Bridle et al. 2008). It was designed to attract new methods from outside the weak lensing community, in particular from computer scientists. Most significantly, the number of galaxies was chosen to test methods at the level required for surveys in the foreseeable future, as calculated in Amara & Réfrégier (2007). A new approach won the competition, inspired by Kuijken (1999), which took advantage of the fact that the same shear was used for many galaxies at a time, by ‘stacking’ the galaxies (Lewis 2009; Hosseini & Bethge 2009). Although progress has been substantial, questions still remain about the likely issues that need to be overcome to reach the precision needed for future all-sky surveys.

In this paper we study noise bias, one of the systematic effects that can affect weak lensing measurements. It arises from high-order noise terms in the measurement of the shape parameters of galaxies, increasing in magnitude at low galaxy signal-to-noise ratio (SNR). Its effects on second order moment measurements from convolved Gaussian galaxy images has been described by Hirata et al. (2004).

To study this effect in a forward-fitting weak lensing measurement context we first derive general expressions for the variance and bias of Maximum-Likelihood Estimators (MLE) of model parameters in the presence of additive

Gaussian noise (§2). We then apply it to a one-parameter toy model consisting of the Maximum-Likelihood (ML) fitting of the size of a Gaussian galaxy model to a Gaussian galaxy convolved with a known Gaussian PSF (§3). While this model is clearly oversimplified it illustrates the principle of noise bias and its amplitude. We then extend this result by considering a more realistic model consisting of an elliptical Gaussian galaxy with 6 free parameters (§4). In §5, we discuss the consequences of our findings and possible remedies, and summarise our conclusions, including a calibration method using simulations discussed in an associated paper (Kacprzak et al. 2012, hereafter K12).

## 2 GENERAL 2D SHAPE ESTIMATION

In this section, we study the general problem of the estimation of the shape parameters of a 2D object in the presence of additive, uncorrelated Gaussian noise. For weak lensing these results are applicable to the measurement of galaxy shapes, and to the estimation of the instrument PSF using stars in the image. The general analytical results that we derive will serve as a useful base for comparison with the more realistic conditions studied by K12 using numerical simulations.

### 2.1 General results

Let us thus consider the observed 2D surface brightness  $f_{\text{obs}}(\mathbf{x})$  of an object that is described by a model  $f(\mathbf{x}; \mathbf{a})$ , where  $\mathbf{x}$  is the position on the image and  $\mathbf{a}$  is the vector of parameters describing the shape of the object. We can write the observed surface brightness as

$$f_{\text{obs}}(\mathbf{x}) = f(\mathbf{x}; \mathbf{a}^t) + n(\mathbf{x}) \quad (1)$$

where  $\mathbf{a}^t$  are the true shape parameters of the object and  $n(\mathbf{x})$  is the noise which is assumed to be uncorrelated and Gaussian with  $\langle n(\mathbf{x}) \rangle = 0$  and  $\langle n(\mathbf{x})^2 \rangle = \sigma_n^2$ .

With these assumptions the log likelihood of the data given the model is  $\ln L = -\chi^2/2$ , where the usual  $\chi^2$ -functional is given by

$$\chi^2(\mathbf{a}) = \sum_p \sigma_n^{-2} [f_{\text{obs}}(\mathbf{x}_p) - f(\mathbf{x}_p; \mathbf{a})]^2, \quad (2)$$

where the sum is over all pixels  $p$  in the image.

The MLE  $\hat{\mathbf{a}}$  for the shape parameters of the object can then be constructed by requiring that  $\chi^2$  is minimised at  $\mathbf{a} = \hat{\mathbf{a}}$ . MLEs were first studied by Fisher (1922), then later by Rao (1973) and Cramér (1999). They are commonly used estimators in statistics and have several desirable properties, including consistency, which requires that in the limit of high SNR the MLE recovers the true values  $\mathbf{a}^t$  of the estimated parameters.

In Appendix A we derive general properties for the MLE  $\hat{\mathbf{a}}$  using an expansion in the inverse SNR of the object. There and in what follows we label SNR using the parameter  $\rho$ . We first show that the covariance of the estimated parameters is, to leading order, given by

$$\text{cov}[\hat{a}_i, \hat{a}_j] = (F^{-1})_{ij} + O(\rho^{-4}), \quad (3)$$

where the Fisher matrix is given by

$$F_{ij} = \sum_p \sigma_n^{-2} \frac{\partial f(\mathbf{x}_p; \mathbf{a}^t)}{\partial a_i} \frac{\partial f(\mathbf{x}_p; \mathbf{a}^t)}{\partial a_j}. \quad (4)$$

We also find that the bias in the parameters  $b[\hat{a}_i] = \langle \hat{a}_i \rangle - a_i^{\text{true}}$  is given by

$$b[\hat{a}_i] = -\frac{1}{2}(F^{-1})_{ij}(F^{-1})_{kl}B_{jkl} + O(\rho^{-4}), \quad (5)$$

where the summation convention over repeated indices is assumed and the bias tensor is given by

$$B_{ijk} = \sum_p \sigma_n^{-2} \frac{\partial f(\mathbf{x}_p; \mathbf{a}^t)}{\partial a_i} \frac{\partial^2 f(\mathbf{x}_p; \mathbf{a}^t)}{\partial a_j \partial a_k}. \quad (6)$$

It is often useful to consider functions  $g_i(\mathbf{a})$  of the parameters. The covariances of these functions are given by

$$\text{cov}[g_i, g_j] = \frac{\partial g_i}{\partial a_k} \frac{\partial g_j}{\partial a_l} \text{cov}[a_k, a_l], \quad (7)$$

while their bias is given by

$$b[g_i] = \frac{\partial g_i}{\partial a_k} b[a_k]. \quad (8)$$

## 2.2 Properties

As can be seen from Equation 5, the bias tensor depends on second order derivatives of the model  $f(\mathbf{x}, \mathbf{a})$  in the parameters  $\mathbf{a}$  and therefore vanishes for linear models. This restates the known fact that MLEs may be biased in general, except in the case of linear models. As noted in Appendix A, the present bias arises from second order noise terms and is therefore referred to as ‘noise bias’.

We then note that the squared error in the parameters  $\sigma^2[a_i] = \text{cov}[a_i, a_i]$  and the bias  $b[a_i]$  are of order

$$b[\hat{a}_i]/a_i^t \sim [\sigma[\hat{a}_i]/a_i^t]^2 \sim \rho^{-2}, \quad (9)$$

in dimensionless units. In the limit of high SNR,  $\rho \rightarrow \infty$ , both tend to zero so that the estimator tends to the true value  $\hat{\mathbf{a}} \rightarrow \mathbf{a}^t$ , thus recovering the consistency property of MLEs (e.g. Cramér 1999).

For finite values of  $\rho$  the statistical error and bias of the parameters can be non negligible. Weak lensing shape measurements are typically performed down to  $\rho \sim 10$  to maximise the surface density of galaxies. In this case, the statistical RMS error will be of order  $\rho^{-1} \sim 0.1$  which is consistent with the typical observed shape noise per galaxy of about  $\delta\gamma \sim 0.3$ , and which includes this statistical measurement error and the distribution of the intrinsic shape of galaxies. The bias in the parameters in this regime will be of order  $\rho^{-2} \sim 0.01$  which is comparable to the weak lensing shear signal  $\gamma \sim 0.02$  and may contribute to explain why some methods do not perform better (e.g. Bridle et al. 2008). As shown by Amara & Réfrégier (2007), the requirement for the variance of the shear systematics is  $\sigma_{sys}^2 \sim 10^{-7}$  which corresponds to the systematic shear error of  $\delta\gamma \sim 3 \times 10^{-4}$ . This is almost two orders of magnitude smaller than predicted by the current analysis of noise bias.

We also note that the expressions for the variance and bias of the ML estimators are expressed in Equations 3 and 5 in terms of a sum over pixel positions, but can often be more conveniently evaluated in the continuum limit where the pixel size is small compared to the object size. This

approximation is given by Equation A8, re-expressing the sum as an integral over the 2D image.

Seemingly counter-intuitively, the bias of the derived parameters  $g_i(\hat{\mathbf{a}})$  is not equal in general to the bias that would be derived had it instead been chosen to find the MLE of the parameters  $\hat{g}_i$  directly. This can be understood from examining the covariance transformation rule described in Equation 7. Thus, the exact value of the bias for any parameter of interest may depend on the parametrisation of the model itself. We will show an example of this property in the following simplified example.

## 3 CIRCULAR GAUSSIAN MODEL

To illustrate the above results, we first consider the case of the measurement of the size of a 2D, circular, Gaussian galaxy without any other free parameters. This is a highly simplified illustration of the shape measurement problem and should therefore be considered as a toy model that captures the main features of the effect of noise bias.

### 3.1 Case without PSF convolution

First, let us consider the case where the galaxy is not convolved with the PSF of the instrument. In this case the galaxy surface brightness is given by

$$f(\mathbf{x}; a) = f_0 \exp \left[ -\frac{r^2}{2a^2} \right], \quad (10)$$

where  $r^2 = x_1^2 + x_2^2$ ,  $f_0$  is a normalization controlling the flux of the galaxy, and  $a$  is the rms size.

To characterise the SNR  $\rho$  of the galaxy, we temporarily consider  $f_0$  as the free parameter while keeping  $a$  fixed. Using the continuum limit (Eq. A8), we can analytically integrate Equation 3 for the variance of the estimator for  $f_0$  and obtain

$$\rho[f_0] = \frac{f_0}{\sigma[f_0]} = \frac{\sqrt{\pi} f_0 a}{\sigma_n h}, \quad (11)$$

where  $h$  is the pixel scale and  $\sigma_n$  is the noise rms as in §2. Here and in the following, we drop the  $\hat{\phantom{x}}$  and  $^t$  symbols to simplify the notation when it does not lead to ambiguities. This definition of the SNR can be considered as the ideal detection signal-to-noise of the galaxy, corresponding to a perfect knowledge of the galaxy shape and position, or equivalently to an ideal matched filter.

Now, considering  $a$  as the only free parameter (and thus leaving  $f_0$  fixed) we again integrate Equation 3 analytically in the continuum limit and obtain

$$\frac{\sigma[a]}{a} = \frac{1}{\sqrt{2}} \rho[f_0]^{-1} + O(\rho^{-2}), \quad (12)$$

which scales as  $\rho^{-1}$  as noted in §2.2. Integrating Equation 5, we find that the bias in this case vanishes at second order, i.e.  $b[a] = 0 + O(\rho^{-4})$ . This is due to a cancelation which we find occurs for any 2D circular galaxy model which can be written as

$$f(\mathbf{x}; a) = f_0 \phi(r/a), \quad (13)$$

where  $\phi$  is any function describing the galaxy profile. Interestingly, this cancelation only occurs in two dimensions,

and the second order bias term does not vanish in 1 or  $> 2$  dimensions even if the above scaling symmetry holds.

### 3.2 Case with PSF convolution

Let us now consider the case of interest in practice where the circular Gaussian galaxy is convolved with a PSF due to the instrument and the atmosphere. In the spirit of the toy model, we make the simplifying assumption that the PSF is itself circular and Gaussian with an rms size  $p$ . Since the convolution of two Gaussians is another Gaussian with standard deviations adding in quadrature, the model in this case is

$$f(\mathbf{x}; a) = f_0 \exp \left[ -\frac{r^2}{2(a^2 + p^2)} \right], \quad (14)$$

where  $f_0$  is a normalization controlling the flux of the galaxy. The PSF size  $p$  is assumed known and the noise assumed to be Gaussian with an rms of  $\sigma_n$ .

In this case, the ideal SNR defined as in §3.1 becomes

$$\rho = \frac{f_0}{\sigma[f_0]} = \frac{\sqrt{\pi} f_0 \sqrt{a^2 + p^2}}{\sigma_n h}, \quad (15)$$

and the uncertainty in the MLE for  $a$  is given by

$$\frac{\sigma[a]}{a} = \frac{1}{\sqrt{2}} \left[ 1 + \left( \frac{p}{a} \right)^2 \right] \rho[f_0]^{-1} + O(\rho^{-2}). \quad (16)$$

Because the presence of the PSF breaks the scaling symmetry of Equation 13, the bias does not vanish to second order and we find

$$\frac{b[a]}{a} = -\frac{1}{4} \left[ 1 + \left( \frac{p}{a} \right)^2 \right] \left( \frac{p}{a} \right)^2 \rho[f_0]^{-2} + O(\rho^{-4}). \quad (17)$$

We note that we recover the results of §3.1 without a PSF when we set  $p = 0$  in the expressions above. We also see that the scalings of Equation 9 hold for the rms error and bias with pre-factors that depend on the ratio of the galaxy to PSF size.

We also notice that if we had instead estimated the convolved galaxy parameters directly, and obtained the deconvolved size as a derived parameter (using Equation 8), the bias would then have vanished to this order. But this would also allow unphysical values of the parameters, with  $a^2 < 0$ . This is an illustration of the fact that the bias of physical parameters depends in general on the specific parametrisation of the estimated model, as discussed in §2.2.

### 3.3 Simulations

In order to check the validity of the expansion described in §2 and Appendix A, and gain insights in the origin of the bias, we performed numerical simulations of this toy model. We considered a range of SNR for a circular Gaussian galaxy of true size  $a^t = 4$  convolved with a circular Gaussian PSF of size  $p = 5.33$  pixels. This corresponds to a ratio of the convolved galaxy size to the PSF size of  $\sqrt{a^{t2} + p^2}/p \simeq 1.25$  which is typically used as the limit for weak lensing surveys.

Even for this very simple one-parameter toy model, we find that great care must be taken for the implementation of the minimization of the  $\chi^2$  function. Readily available

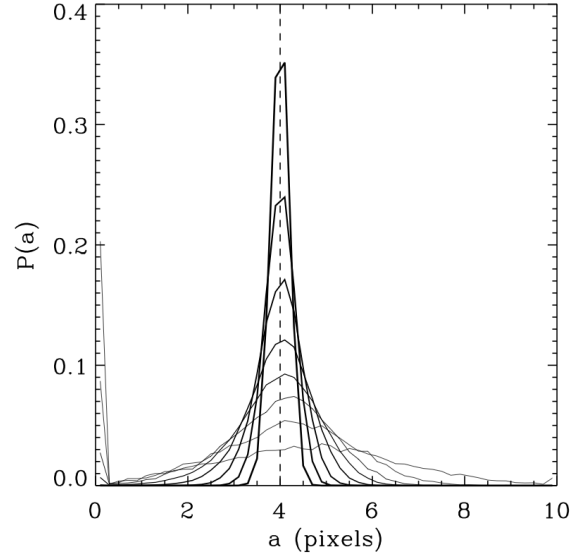


**Figure 1.** Distribution  $P(a)$  of the MLE estimator for the size  $a$  of the 2D Gaussian from repeated realisations. The curves from broad (thin lines) to sharp (thick lines) correspond to SNR  $\rho[f_0]$  of 3, 5, 7, 9, 12, 17, 25, 40, respectively. The true value of the parameter  $a^t = 4$  pixels is shown as the vertical dashed line. The PSF size is  $p = 5.33$  pixels corresponding to a convolved galaxy size to the PSF size of  $\sqrt{a^{t2} + p^2}/p \simeq 1.25$ .

minimiser algorithms produced artifacts that appear to depend on the choice of algorithm at the high level of precision required for weak lensing. For the present simulations, we computed  $\chi^2(a)$  on a grid in the interval  $0.1 < a < 10$  pixels with a grid size of  $\Delta a = 0.0033$  pixels and found the minimum by direct search.

Figure 1 shows the resulting Probability Distribution Function (PDF)  $P(a)$  of the estimator for  $a$  for a range of SNR  $\rho[f_0]$ . At high SNR, the PDF is nearly Gaussian and peaks close to the true value  $a^t = 4$  pixels. As the SNR decreases, the PDF main peak shifts towards the right, while a secondary peak at  $a = 0$  starts developing. The complicated combination of these two effects contribute to the dependence of the bias and rms error on SNR.

Figure 2 shows the dependence of the rms variance  $\sigma[a]$  on the SNR  $\rho[f_0]$ . We see that our expression in Equation 3 is a good approximation for  $\rho[f_0] \gtrsim 10$ . The deviations below this value are not surprising since higher order terms are expected to become important in the low SNR limit.

Figure 3 shows the dependence of the bias  $b[a]$  on the SNR  $\rho[f_0]$ . Again, our expression in Equation 5 is a good approximation for SNR  $\gtrsim 10$ , with deviations below this value likely due to higher order terms. The horizontal, dashed line in the lower panel corresponds to the requirement for future all sky surveys  $b[a]/a \simeq \delta\gamma \simeq 3 \times 10^{-4}$  as discussed in §2.2 and in Amara & Réfrégier (2007). The bias for galaxies with SNR  $\sim 10$  in this toy model is  $b[a]/a \simeq 0.015$ , which is nearly two order of magnitude greater than this requirement and comparable to the expected weak lensing signal  $\delta\gamma \simeq 0.02$ .

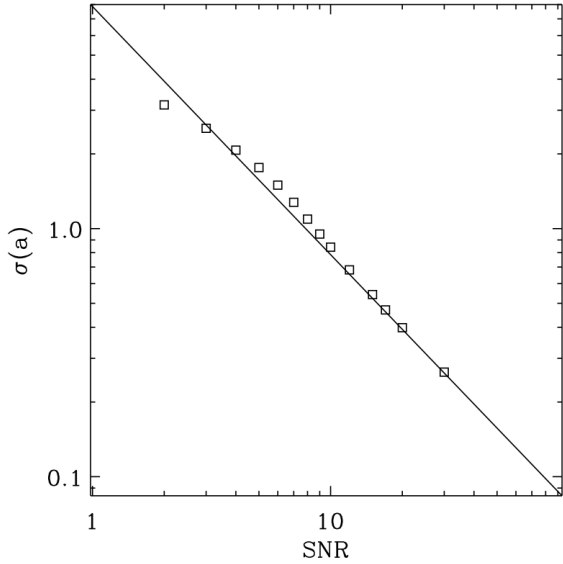


**Figure 2.** Standard deviation  $\sigma[a]$  of the size estimator  $a$  as a function of signal-to-noise ratio  $\text{SNR} = \rho[f_0]$ . The expectation from the analytical prediction (solid line) is compared to the measurements from repeated experiments.

#### 4 ELLIPTICAL GAUSSIAN MODEL

We now consider a slightly more realistic model of a galaxy consisting of a 2D elliptical Gaussian galaxy with 6 parameters. This is the smallest number of parameters needed to measure galaxy shapes for weak lensing in practice as they correspond to the 2 centroid coordinates, flux, major and minor axes and position angle of the galaxy. In practice the models for galaxies are typically non-Gaussian and more complicated in order to better describe realistic galaxies. The 6-parameter Gaussian model is nevertheless useful to study the behaviour of the bias in the multi-parameter case.

Let us thus consider a galaxy surface brightness given by a 2D elliptical Gaussian (without PSF convolution) that we parametrise as (see also Paulin-Henriksson et al. 2008 for a slightly different parametrisation):

$$f(\mathbf{x}; \mathbf{a}) = \frac{A}{2\pi\sqrt{a_1 a_2}} \exp \left[ -\frac{1}{2}(\mathbf{x} - \mathbf{x}^a)^T \mathbf{A}^{-1}(\mathbf{x} - \mathbf{x}^a) \right], \quad (18)$$

where  $a_1$  and  $a_2$  are the (rms) major and minor axes of the Gaussian respectively,  $A$  is a parameter which determines the amplitude,  $\mathbf{x}^a$  is the centroid, and  $^T$  denotes the transpose operator. The quadrupole moment matrix  $\mathbf{A}$  is a  $2 \times 2$  symmetric matrix which can be written as

$$\mathbf{A} = \mathbf{R}(\alpha)^T \begin{pmatrix} a_1^2 & 0 \\ 0 & a_2^2 \end{pmatrix} \mathbf{R}(\alpha), \quad (19)$$

where  $\alpha$  is the position angle of the major axis counter-clockwise from the  $x$ -axis and

$$\mathbf{R}(\alpha) = \begin{pmatrix} \cos \alpha & \sin \alpha \\ -\sin \alpha & \cos \alpha \end{pmatrix} \quad (20)$$

is the rotation matrix which aligns the coordinate system with the major axis. In Appendix B, we show that the amplitude, centroid, and quadrupole moment matrix are simply

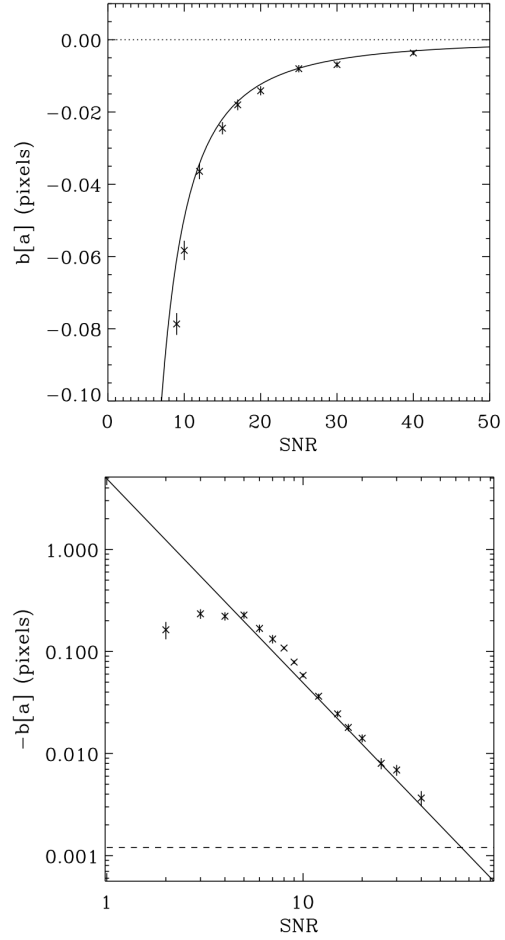


**Figure 3.** Bias  $b[a]$  of the size estimator  $a$  as a function of  $\text{SNR} = \rho[f_0]$  in linear (upper panel) and log (lower panel) axes. In both panels, the solid line correspond to the analytical model while the squares were derived from simulations of repeated experiments. The horizontal dashed line in the bottom panel corresponds to the requirement for future all sky surveys (see text).

related to the multipole moments of galaxy surface brightness.

Let us consider the MLEs for this 2-dimensional Gaussian with the following 6 free parameters

$$\mathbf{a} = (x_1^a, x_2^a, A, a_1, a_2, \alpha). \quad (21)$$

In the continuum limit (Eq. A8), the Fisher matrix equations (4) can be computed analytically. This is facilitated by rotating into the coordinate system aligned with the major and minor axes of the galaxy, before performing the integral of the surface of the galaxy. The resulting Fisher matrix  $F_{ij}$  and covariance matrix  $\text{cov}[a_i, a_i]$  of the parameters are given in Equation B4 in Appendix B. We note that, with this parametrisation, the Fisher matrix is conveniently nearly diagonal<sup>1</sup>. The corresponding rms statistical errors

<sup>1</sup> Note that in the parametrisation of Paulin-Henriksson et al. (2008) the Fisher matrix is also not quite diagonal, due to covariance terms between their rotated centroid and the position angle neglected in this paper.

$\sigma[a_i] = \text{cov}[a_i, a_i]^{1/2}$  are listed in the third column in the top part of Table 1, to leading order in the SNR of the amplitude  $A$ , defined as

$$\rho[A] \equiv \frac{A}{\sigma[A]} = \frac{A}{\sqrt{4\pi h \sigma_n}}. \quad (22)$$

Using Equation (5) after the same change of coordinates and some cumbersome algebra, we can also derive the bias in the model parameters which are given in Equation B5 and listed in the last column of Table 1. Note that several of the parameters have a singularity as the galaxy becomes circular, i.e. when  $\epsilon = 0$ , which occurs at  $a_1 = a_2$ . This follows from the fact that, in this limit, the position angle  $\alpha$  becomes degenerate.

From these expressions, and using Equations (7-8), we can derive the error and bias for derived quantities. The lower part of Table 1 provides the definition, statistical errors and biases for several commonly used parameters such as the flux  $F^{(0)}$  (see also Equation B1), the average radius  $a = \sqrt{a_1^2 + a_2^2}$  and two definitions of the ellipticities  $\epsilon$  and  $e$ . All these parameters are biased to second order in  $\rho[A]$ . Interestingly, the average radius  $a$  is biased in the elliptical case even in the absence of a PSF convolution, as a result of covariances with other parameters. Also, it is interesting to note that the rms error and bias of  $a_1$  and  $a_2$  have a singularity in the circular case, but that the singularity cancels when they are combined to form the mean radius  $a$ . We can also verify that the scaling of Equation 9 for the variance and bias of the parameters holds up to multiplicative factors of order unity.

## 5 CONCLUSIONS

In this paper we have studied the effect of noise bias on MLEs for weak lensing shape parameters in the presence of additive Gaussian noise. We have derived general expressions for the covariance and bias for ML-estimated parameters of 2D galaxy images, which are given by Equations 3 and 5. The bias vanishes for linear models, but is generally non-zero for models which are non-linear in the parameters and depend on the model parametrisation. To illustrate the effect of the noise bias we have calculated analytical expressions for the variance and bias for a toy model consisting of a 2D circular Gaussian galaxy, convolved with a circular Gaussian PSF, with the galaxy size as a single free parameter. We have compared these predictions with careful numerical simulations and found them to be in good agreement. We also provide analytical results for a 2D elliptical Gaussian with 6-parameters.

We find that the variance and bias of the parameters are generically of order  $\rho^{-2}$ , where  $\rho$  is the SNR of the galaxies. For galaxies with  $\rho \sim 10$ , which is typical of weak lensing surveys, this implies a bias in the parameters of order  $\rho^{-2} \sim 0.01$ . This is comparable to the weak lensing shear signal  $\gamma \sim 0.02$  and nearly two orders of magnitude greater than the systematic shear tolerance required for future all sky surveys,  $\delta\gamma \sim 3 \times 10^{-4}$ . Although derived using the specific case of the MLE in the presence of Gaussian noise, our results are likely to be generic across a number of measurement techniques. This may contribute towards explaining why current weak lensing surveys are limited by systemat-

ics, and why finding sufficiently accurate methods has been difficult.

To solve this problem, the following ways forward are possible

- Use higher SNR galaxies. This is an obvious solution but it is costly in practice as it leads to a sharp drop in the useful surface density of galaxies, or requires longer exposure times and/or larger telescopes.
- Avoid non-linearities, either by choosing linear models or using moment-based methods. This was the idea behind shapelets methods, but we note that in all cases some level of non-linearity is unavoidable as the centroid and size (of the basis functions or weight function) are intrinsically non-linear.
- Go beyond ML estimation by using, e.g., Bayesian methods or other averaging techniques. For instance, the introduction of stacking methods was a breakthrough in the GREAT08 challenge (Bridle et al. 2008).
- Calibrate the bias. While order-by-order correction methods exist for the MLEs, the models used in practice to model galaxies (e.g., exponential, de Vaucouleur, Sérsic, or a multi-component combination) convolved with observed PSFs will be complex and thus not offer analytical expressions for the bias. Instead, numerical simulations will be needed for the bias calibration. This is the approach described in the accompanying paper by Kacprzak et al. (2012).

We thank Gary Bernstein, Julien Carron, Joël Bergé, Stéphane Paulin-Henriksson and Lisa Voigt for helpful discussions. Sarah Bridle acknowledges support from the Royal Society in the form of a University Research Fellowship, and both Sarah Bridle and Barnaby Rowe acknowledge support from the European Research Council in the form of a Starting Grant with number 240672. Part of Barnaby Rowe's work was done at the Jet Propulsion Laboratory, California Institute of Technology, under contract with NASA.

## REFERENCES

- Albrecht A., Bernstein G., Cahn R., Freedman W. L., Hewitt J., Hu W., Huth J., Kamionkowski M., Kolb E. W., Knox L., Mather J. C., Staggs S., Suntzeff N. B., 2006, ArXiv Astrophysics e-prints
- Amara A., Réfrégier A., 2007, MNRAS, 381, 1018
- Bernstein G. M., 2010, MNRAS, 406, 2793
- Bernstein G. M., Jarvis M., 2002, AJ, 123, 583
- Bonnet H., Mellier Y., Fort B., 1994, ApJ, 427, L83
- Bridle S., Kneib J.-P., Bardeau S., Gull S., 2002, in Natarajan P., ed., The shapes of galaxies and their dark halos, Proceedings of the Yale Cosmology Workshop "The Shapes of Galaxies and Their Dark Matter Halos", New Haven, Connecticut, USA, 28-30 May 2001. Edited by Priyamvada Natarajan. Singapore: World Scientific, 2002, ISBN 9810248482, p.38 Bayesian galaxy shape estimation. pp 38+
- Bridle et al. 2008, ArXiv e-prints
- Cramér H., 1999, Mathematical methods of statistics. Princeton landmarks in mathematics and physics, Princeton University Press

**Table 1.** Statistical errors and biases of parameters for 6-parameter elliptical Gaussian model. Errors and biases are shown to leading order in  $\rho$

Parameter Name	Symbol $a$	Stat. Error $(\sigma[a]/a)\rho[A]$	Bias $(b[a]/a)\rho[A]^2$
Model Parameters			
Centroid	$x_1^a$	$\sqrt{2(a_1^2 \cos^2 \alpha + a_2^2 \sin^2 \alpha)}/x_1^a$	0
Centroid	$x_2^a$	$\sqrt{2(a_2^2 \cos^2 \alpha + a_1^2 \sin^2 \alpha)}/x_2^a$	0
Amplitude	$A$	1	5/2
Major axis	$a_1$	$\sqrt{2}$	$\epsilon^{-1}$
Minor axis	$a_2$	$\sqrt{2}$	$-\epsilon^{-1}$
Position angle	$\alpha$	$2\sqrt{\epsilon^{-2} - 1}/\alpha$	0
Derived Parameters			
Flux	$F^0 = A\sqrt{a_1 a_2}$	$\sqrt{2}$	5/2
Radius mean	$a = \sqrt{a_1^2 + a_2^2}$	$\sqrt{1 + \epsilon^2}$	1
Ellipticity (quadratic)	$\epsilon = \frac{a_1^2 - a_2^2}{a_1^2 + a_2^2}$	$2(1 - \epsilon^2)/\epsilon$	$2(1 - \epsilon^2)/\epsilon^2$
Ellipticity (linear)	$e = \frac{a_1 - a_2}{a_1 + a_2}$	$(1 - e^2)/e$	$(1 - e^4)/(2e^2)$

- Fisher R. A., 1922, Philosophical Transactions of the Royal Society of London. Series A, Containing Papers of a Mathematical or Physical Character, 222, pp. 309
- Heymans et al. 2006, MNRAS, 368, 1323
- Hirata C. M., Mandelbaum R., Seljak U., Guzik J., Padmanabhan N., Blake C., Brinkmann J., Budávári T., Connolly A., Csabai I., Scranton R., Szalay A. S., 2004, MNRAS, 353, 529
- Hoekstra H., Jain B., 2008, Annual Review of Nuclear and Particle Science, 58, 99
- Hosseini R., Bethge M., 2009, Max Planck Institute for Biological Cybernetics Technical Report
- Kaiser N., 2000, ApJ, 537, 555
- Kaiser N., Squires G., Broadhurst T., 1995, ApJ, 449, 460
- Kuijken K., 1999, A&A, 352, 355
- Lewis A., 2009, MNRAS, 398, 471
- Massey et al. 2007, MNRAS, 376, 13
- Melchior P., Böhnert A., Lombardi M., Bartelmann M., 2010, A&A, 510, A75
- Miller L., Kitching T. D., Heymans C., Heavens A. F., van Waerbeke L., 2007, MNRAS, 382, 315
- Paulin-Henriksson S., Amara A., Voigt L., Refregier A., Bridle S. L., 2008, A&A, 484, 67
- Paulin-Henriksson S., Refregier A., Amara A., 2009, A&A, 500, 647
- Peacock J., Schneider P., 2006, The Messenger, 125, 48
- Rao C., 1973, Linear statistical inference and its applications. Wiley series in probability and mathematical statistics. Probability and mathematical statistics, Wiley
- Refregier A., 2003, ARA&A, 41, 645
- Refregier A., Bacon D., 2003, MNRAS, 338, 48
- Rowe B., 2010, MNRAS, 404, 350
- Tyson J. A., Wenk R. A., Valdes F., 1990, ApJ, 349, L1
- Voigt L. M., Bridle S. L., 2010, MNRAS, 404, 458

## APPENDIX A: BIAS FOR GENERAL MLE

In this Appendix, we provide the derivation of the main results for the variance and bias of a general MLE of parameters given in §2 for additive, uncorrelated Gaussian noise. For the model describe in §2, the likelihood is

$$L \propto e^{-\chi^2/2} \quad (\text{A1})$$

where

$$\chi^2(\mathbf{a}) = \sum_p \sigma_n^{-2} [f(\mathbf{x}_p; \mathbf{a}^t) + n(\mathbf{x}_p) - f(\mathbf{x}_p; \mathbf{a})]^2. \quad (\text{A2})$$

The MLE  $\hat{\mathbf{a}}$  is then defined as the value of the parameters  $\mathbf{a}$  which maximises the likelihood  $L$  or, equivalently, which minimises  $\chi^2$ , i.e. for which

$$\left. \frac{\partial \chi^2}{\partial \mathbf{a}} \right|_{\hat{\mathbf{a}}} = 0. \quad (\text{A3})$$

To proceed, we expand this expression in terms of the inverse of the SNR,  $\rho \sim f/n$ , of the object. This can be conveniently done by rewriting  $n(\mathbf{x}_p) \rightarrow \alpha n(\mathbf{x}_p)$  and  $\hat{\mathbf{a}} = \mathbf{a}^t + \alpha \delta \mathbf{a}^{(1)} + \alpha^2 \delta \mathbf{a}^{(2)} + \dots$ , where  $\alpha$  is a dimensionless order parameter which scales as  $\alpha \sim \rho^{-1}$ . We then Taylor expand  $f(x, a)$  about  $a^t$ , collect like powers of  $\alpha$  in Equation A3, and set  $\alpha = 1$ . The terms of order  $\alpha$  yield

$$\delta a_i^{(1)} = (F^{-1})_{ij} \sum_p \sigma_n^{-2} n(\mathbf{x}_p) \frac{\partial f(\mathbf{x}_p; \mathbf{a})}{\partial a_j}. \quad (\text{A4})$$

where the fisher matrix  $F_{ij}$  was defined in Equation 4. Taking the average of this expression and using the fact that the noise is unbiased, i.e.  $\langle n(\mathbf{x}_p) \rangle = 0$ , we see that the estimator is unbiased to this order. Taking the average of the product  $\langle \delta a_i^{(1)} \delta a_j^{(1)} \rangle$  and using the fact that the noise is uncorrelated, i.e.  $\langle n(\mathbf{x}_p) n(\mathbf{x}_{p'}) \rangle = \delta_{p,p'} \sigma_n^2$ , we obtain the expression for the covariance of the parameters to leading order given in Equation 3.

The terms of order  $\alpha^2$  yield

$$\delta a_i^{(2)} = -\frac{1}{2} (F^{-1})_{ij} (F^{-1})_{kl} B_{jkl}, \quad (\text{A5})$$

and thus gives Equation 5 for the bias to leading order, where the bias tensor was defined in Equation 6.

These results can also be derived from the general expressions of the Fisher Matrix

$$F_{ij} = \left\langle -\frac{\partial^2 \ln L}{\partial a_i \partial a_j} \right\rangle \quad (\text{A6})$$

and for the bias tensor for the MLE

$$B_{ijk} = \left\langle -\frac{1}{2} \frac{\partial^3 \ln L}{\partial a_i \partial a_j \partial a_k} + \frac{\partial \ln L}{\partial a_j} \frac{\partial^2 \ln L}{\partial a_i \partial a_k} \right\rangle. \quad (\text{A7})$$

In the limit of small pixels, the sum over pixels in the expressions above can be approximated by a continuous integral

$$\sum_p \simeq \int \frac{d^2 x}{h^2}, \quad \text{as } h \rightarrow 0, \quad (\text{A8})$$

where  $h$  is the pixel size.

## APPENDIX B: RESULTS FOR THE ELLIPTICAL GAUSSIAN MODEL

In this Appendix, we provide results for the elliptical Gaussian model defined in Equation 18 as a function of the 6 parameters listed in Equation 21 in the presence of additive, uncorrelated Gaussian noise as defined in Equation 1.

With this parametrisation, the flux, or zeroth order moment of the Gaussian is given by

$$F^{(0)} = \int d^2 x f(\mathbf{x}; \mathbf{a}) = A\sqrt{a_1 a_2}. \quad (\text{B1})$$

The centroid, or first order moments are given by

$$\frac{F_i^{(1)}}{F^{(0)}} = \frac{1}{F^{(0)}} \int d^2 x x_i f(\mathbf{x}; \mathbf{a}) = x_i^a, \quad (\text{B2})$$

and the quadrupole moment matrix, containing the second order moments, is given by

$$\frac{F_{ij}^{(2)}}{F^{(0)}} = \frac{1}{F^{(0)}} \int d^2 x x_i x_j f(\mathbf{x}; \mathbf{a}) = A_{ij}. \quad (\text{B3})$$

For this model, in the continuum limit (Eq. A8), the Fisher Matrix  $F_{ij}$  (Eq. 4) can be derived analytically by rotating into a coordinate system with axes parallel to the major and minor axes of the galaxy (using the rotation matrix in Eq. 20) before performing the integrals over the surface of the galaxy. The covariance matrix of the parameters is then obtained by inverting the Fisher matrix (Eq. 3) which yields

$$\text{cov}[\hat{a}_i, \hat{a}_j] = \begin{pmatrix} 2A_{11} & 2A_{12} & 0 & 0 & 0 & 0 \\ 2A_{12} & 2A_{22} & 0 & 0 & 0 & 0 \\ 0 & 0 & A^2 & 0 & 0 & 0 \\ 0 & 0 & 0 & 2a_1^2 & 0 & 0 \\ 0 & 0 & 0 & 0 & 2a_2^2 & 0 \\ 0 & 0 & 0 & 0 & 0 & \frac{4a_1^2 a_2^2}{(a_1^2 - a_2^2)^2} \end{pmatrix} \times \rho[A]^{-2} + O(\rho^{-3}), \quad (\text{B4})$$

where  $A_{ij}$  are the components of the quadrupole moment matrix  $\mathbf{A}$  defined in Equation 19, and  $\rho[A]$  is the SNR of the amplitude  $A$  given in Equation 22.

The bias in the parameters can be derived using Equation 5 which yields

$$\frac{b[a_i]}{a_i} = \left(0, 0, \frac{5}{2}, \epsilon^{-1}, -\epsilon^{-1}, 0\right) \rho[A]^{-2} + O(\rho^{-3}), \quad (\text{B5})$$

where the quadratic ellipticity  $\epsilon$  is defined in Table 1.

The resulting rms errors and biases for the model parameters are summarised in the upper part of Table 1.